

Binding energy of the free exciton in indium arsenide

P. J. P. Tang, M. J. Pullin, and C. C. Phillips

Physics Department, The Blackett Laboratory, Imperial College of Science, Technology and Medicine, Prince Consort Road, London SW7 2BZ, United Kingdom

(Received 26 April 1996)

We report the 0–5 T magnetoabsorption spectra of high-quality InAs epilayers grown by molecular-beam epitaxy on GaAs. Excitonic absorption is observed at all fields, and, from the absolute energy of the magnetoexciton absorption peak, the zero-field exciton binding energy is found to be in excellent agreement with the theoretical prediction of 1.0 meV from calculations which take into account the anisotropy, degeneracy, and spin splitting of the InAs band structure. The energy shift of the magnetoexciton at high fields is found to agree with predicted shifts using the adiabatic method. [S0163-1829(97)03707-7]

I. INTRODUCTION

The narrow band gap of InAs (0.35 eV at 300 K) and its high electron mobility have drawn considerable interest for many technological applications including high-speed electronic devices, saturable absorbers for gain-switching infrared lasers,¹ and infrared detectors and emitters.² InAs is a constituent of many important quantum-well structures, for example, InAs/GaSb superlattices which exhibit important crossed gap properties. It has also recently been demonstrated that strained-layer superlattices composed of alternating InAs and InAs_{1-x}Sb_x layers can produce room-temperature long-wavelength 4–11 μm infrared emitters.^{3,4}

Compared with wider-band-gap III-V semiconductors, few spectroscopic studies of InAs exist. The nature of the states introduced by various impurity species is not well understood, and this complicates the extraction of exciton binding energy values from photoluminescence (PL) data, since the spectra are likely to be dominated by transitions involving impurity states of unknown energies. Here we determine the exciton binding energy from magnetoabsorption data. These are effectively density-of-states measurements, and impurity-related transitions have a negligible influence. This contrasts with PL measurements, which strongly emphasize the lowest-energy states (usually impurity related), since the thermalization time of electrons and holes to these states is much shorter than the recombination time of higher-energy band-to-band transitions.

The high exciton density of states gives strong free-exciton absorption transitions in InAs, provided the background carrier concentration is low enough to prevent electron-hole screening of the exciton state. The sample studied here was grown on GaAs which is transparent over the required wavelength range, but leads to high defect densities (estimated to be $\sim 1 \times 10^9 \text{ cm}^{-2}$) (Ref. 5) due to the large (7%) InAs/GaAs lattice mismatch. In most III-V semiconductors this defect density would suppress free-exciton transitions by generating localized charged defect states which give rise to random Coulomb fields, effectively field ionizing the excitons and giving a featureless ‘‘Urbach tail’’ in the absorption spectrum. InAs, however, appears to be unique among the III-V’s in that pointlike defects form energy states in the conduction band as opposed to Shockley-Read defect

centers in the band gap.⁶ This is consistent with the well-known pinning of the electron Fermi level high in the conduction band at the InAs/vacuum interface (where surface states can be regarded as extreme cases of point defects) leading to a native electron accumulation layer. Thus even though defect densities may be high here, their adverse influence on excitonic transitions appears to be negligible.

We identify free excitons whose binding energy is much less than previously reported values,^{7,8} and we show that this binding-energy value agrees with theoretical predictions in the zero-field and high magnetic-field limits proposed by Baldereschi and Lipari⁷ and Altarelli and Lipari,⁹ respectively.

II. EXPERIMENTAL DETAILS

The 5- μm -thick InAs epilayer was grown by molecular beam epitaxy (MBE) on a (100)-oriented GaAs substrate.¹⁰ Following desorption of the oxide passivation layer on the substrate, a 0.5- μm GaAs buffer layer was grown at a substrate temperature of $\approx 550^\circ\text{C}$. The InAs epilayer was grown under As-rich conditions with an As to In flux ratio of 2.4, and a growth rate of $0.57 \mu\text{m h}^{-1}$. These values were calibrated by the reflection high-energy electron-diffraction oscillation technique. X-ray-diffraction measurements at room temperature indicate that the InAs layer is strain relaxed to better than 3 in 10^6 . On the basis of the known thermal-expansion coefficients of InAs and GaAs, this would result in a 4.2-K band-gap shift of at most $50 \mu\text{eV}$, entirely negligible for our purposes. This is corroborated by the absence of strain-split transitions for the InAs epilayers over all the field strengths studied. Moreover, electron and hole masses of $0.023m_0$ and $0.4m_0$, respectively, have been extracted from this epilayer, which are close to the literature values.¹¹ These experimental mass values were obtained by fitting the Pidgeon-Brown model (without strain) to high Landau levels where the magnetoexciton perturbation is extremely small compared to the large cyclotron energies.¹² The masses were derived from accurate fits to over 10 different Landau levels. We are thus confident that the InAs epilayer of this study is entirely strain relaxed.

A simpleminded interpretation of the Hall data from this sample would suggest an overall Hall mobility of 81 000

$\text{cm}^2 \text{V}^{-1} \text{s}^{-1}$ at 77 K,¹⁰ but the pinning of the Fermi energy by surface states ≈ 300 meV above the conduction-band edge^{6,13} is known to produce a low-mobility ($\sim 10^4 \text{ cm}^2 \text{V}^{-1} \text{s}^{-1}$) two-dimensional electron gas (2DEG) at the surface. Including this 2DEG in a two-carrier fit to the Hall data yields a bulk 77-K mobility of $200\,000 \text{ cm}^2 \text{V}^{-1} \text{s}^{-1}$ and a bulk carrier concentration of $2 \times 10^{14} \text{ cm}^{-3}$.

This was corroborated by far-infrared magnetophotocconductivity measurements, which showed a broad cyclotron-resonance (CR) line associated with the 2DEG which had the expected $1/\cos\theta$ resonance energy dependence as the sample was tilted at angle θ to the magnetic field.¹⁰ On top of this was an extremely sharp cyclotron-resonance line (with a width comparable to high-quality GaAs epilayers) that did not shift with θ . Fitting its linewidth and absorption coefficient gave independent estimates of the 4.2-K bulk carrier concentration and mobility of $< 5 \times 10^{14} \text{ cm}^{-3}$ and $> 300\,000 \text{ cm}^2 \text{V}^{-1} \text{s}^{-1}$, respectively.

Impurity-shifted cyclotron-resonance (CR) lines were also seen, indicating the presence of shallow donors with a binding energy of ~ 1 meV. These small impurity binding energies resulted in incomplete freeze-out, leaving the small residual carrier concentration even at 4.2 K (when $kT=0.36$ eV) which allowed the observation of CR and ICR lines. The 77-K Hall mobilities and magnetoresistance of this sample (measured without illumination) were similar to a number of samples grown in the same MBE machine, all of which had bulk carrier concentrations^{10,14} of the order of $2 \times 10^{14} \text{ cm}^{-3}$. It is difficult to identify the particular impurity species responsible for the small carrier concentration. A splitting of the $(1s-2p_-)$ ICR line due to differences in central cell corrections for two different impurity species does show that more than one type of donor is present, but it has yet to be identified with certainty whether this is due to carbon and/or the contaminants present in the MBE source materials like sulfur or selenium. In any case the experimental evidence clearly shows that we have one of the purest InAs samples ever reported, and the fact that ICR lines can be observed indicates that the Fermi energy is well below the conduction-band edge.

The sample was mounted together with a cadmium mercury telluride detector (sensitive out to $14 \mu\text{m}$) in a steel insert filled with He heat exchange gas. The insert was placed in a superconducting solenoid (with a maximum magnetic field strength of 5 T) within a liquid-He Dewar. The sample was oriented in the Faraday configuration, and was mounted strain free. Transmission spectra were obtained by using modulated unpolarized light from a Bomem Fourier Transform spectrometer which was directed via highly polished light pipes to the sample.

III. RESULTS AND DISCUSSION

The 4.2-K magnetoabsorption spectra are shown in Fig. 1. There is a clear absorption feature (centered at 418.2 meV) even at zero field. We note that the previous observation of several ICR lines in this epilayer with similar absorption strengths to the CR line¹⁴ indicates that the Fermi energy is well below the conduction-band edge at 4.2 K over the field range of interest, and that the impurity concentration is below the metal-insulator transition concentration as required

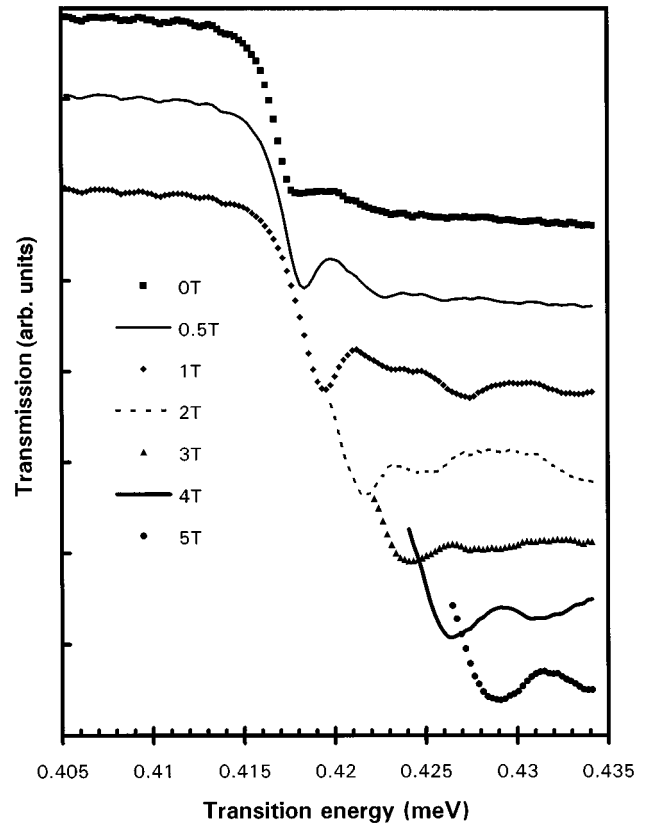


FIG. 1. Magnetoabsorption spectra of a $5\text{-}\mu\text{m}$ InAs epilayer on GaAs at various fields in the range 1–5 T.

for the observation of free excitons. The lower-energy bound-exciton transitions that appear in the PL spectrum of this sample¹⁵ are absent in the absorption spectra (Fig. 1). In addition, picosecond pump-probe measurements of the recombination dynamics¹⁶ show that dislocations in the bulk of the layer have negligible effect on carrier recombination.

On account of these and the considerations of Sec. I, we conclude that this absorption feature cannot be defect related. All the evidence is consistent with it being a free-exciton absorption feature, and we model its magnetic-field dependence on this basis.

Previous magneto-PL studies of InAs have been described in terms of electron-heavy-hole excitonic transitions, but without the effects of spin splitting of the conduction- and valence-band states^{8,17} being taken into account. In our present study, the exciton absorption peak broadens with increasing field, suggesting that it could be composed of heavy-hole exciton states which are degenerate at zero field but spin-split by the magnetic field. Previous studies have revealed higher Landau transitions as a consequence of higher magnetic fields used (8 T); the purpose of the present magnetoabsorption study is partly to show the unique low field shift of excitons in InAs (Fig. 2) compared to linear shifts of free carrier transitions. Figure 1 does show a 431-meV light-hole transition at 4 T which corresponds well to previous higher field observations, but this transition is very weak at lower fields, and the spectra are dominated by heavy-hole exciton transitions. Figure 2 shows the magnetic shift of the exciton together with the theoretical energy shifts (calculated as described below) of the allowed heavy-hole

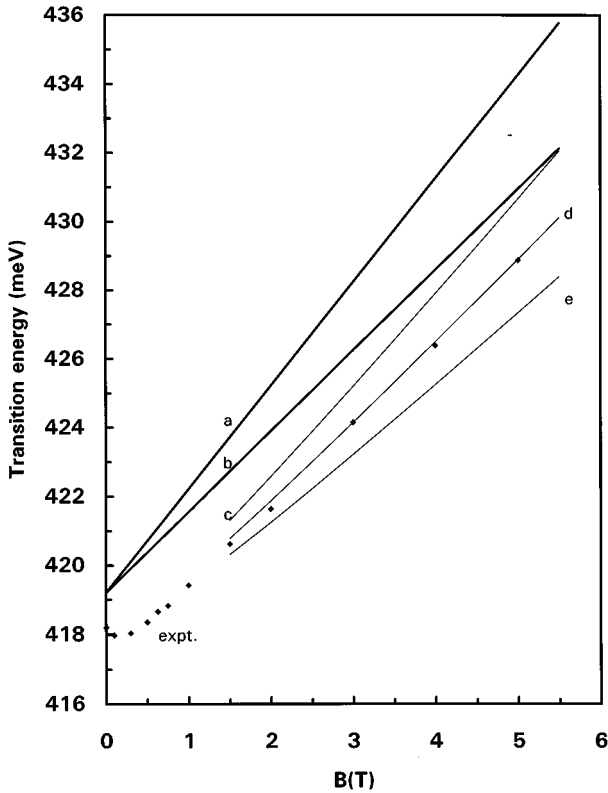


FIG. 2. \blacklozenge : Experimental magnetoabsorption peak positions. Solid lines: theoretical curves for the various heavy-hole to conduction-band transitions. (a) $hh\downarrow-e\downarrow$ band to band. (b) $hh\uparrow-e\uparrow$ band to band. (c) $hh\downarrow-e\downarrow$ magnetoexciton. (d) $hh-e$ magnetoexciton transition with no spin splitting. (e) $hh\uparrow-e\uparrow$ magnetoexciton.

transitions from the degenerate valence band to spin-up and spin-down conduction-band states.

At low field $B < 1$ T, where the cyclotron energy is much less than the InAs band gap, and the parabolic approximation holds, the Landau levels and hence the band-to-band transition energies shift linearly with field. The lack of shift in the experimental data (Fig. 1) is characteristic of an excitonic transition^{18,19} in the low-field regime, i.e., where the cyclotron energy is less than the binding energy of the free exciton (the excitonic Rydberg), the exciton Hamiltonian closely resembling that of a hydrogen atom in a magnetic field. Zeeman splitting causes a fanning out of opposing spin states below and above the zero-field degenerate level. At higher fields a quadratic diamagnetic shift is observed, due to the induced magnetic moment of the exciton interacting with the magnetic field. The sum of the diamagnetic and Zeeman shift terms is, however, rather less than the shifts of the free-carrier Landau levels. In the following analysis we interpret the data for both the zero- and high-field cases, and show that they give mutually compatible values for the exciton binding energy.

A. Zero-field exciton binding energy

The zero-field exciton binding energy in a semiconductor with an anisotropic valence band can be derived from perturbation theory using hydrogenic wave functions. The exciton Hamiltonian can be expressed as⁷

TABLE I. Band parameters for InAs (Refs. 19 and 20).

$\gamma_1 = 19.67$
$\gamma_2 = 8.37$
$\gamma_3 = 9.29$
$g = 14.7$
$\kappa = 7.68$
$q = 0.04$
$m_e^* = 0.023m_0$
$\epsilon_r = 15.15$
$\Delta = 0.38$ eV

$$H_{\text{ex}} = H_s + H_d, \quad (1)$$

where H_s represents the interaction between the electron and the isotropic part of the hole and H_d represents the anisotropy in the valence band derived from the Luttinger-Kohn Hamiltonian.²⁰ Their explicit expressions for a crystal with a diamond structure have been derived by Baldereschi and Lipari.⁷

H_s is a 6×6 diagonal matrix. Four of the terms are

$$P = \frac{p^2}{2\mu_0} - \frac{e^2}{4\pi\epsilon_0\epsilon_r r}, \quad (2)$$

with

$$\frac{1}{\mu_0} = \frac{1}{m_e^*} + \frac{\gamma_1}{m_0}, \quad (3)$$

where m_e is the electron effective mass and γ_1 is the usual Luttinger parameter (given in Table I). P represents the Coulomb interaction between the electron and the isotropic part of the heavy- and light-hole bands with two different spin orientations. The remaining two terms in H_s are the same as in Eq. (2), but with the addition of the spin-split-off energy term. H_s is much larger than H_d , since the latter does not contain the electron effective mass in the denominator of the momentum matrix elements like Eq. (2).

P represents the hydrogenic Hamiltonian with a reduced effective mass μ_0 and dielectric constant $\epsilon_0\epsilon_r$, and H_s can be solved exactly to give the familiar hydrogeniclike eigenvalues and eigenfunctions. The eigenstates of H_s consist of a fourfold-degenerate series and a twofold-degenerate state series separated by the spin-orbit splitting Δ , both series having the same effective Rydberg,

$$R_0 = \frac{\mu_0 e^4}{2(4\pi\epsilon_0\epsilon_r)^2 \hbar^2}, \quad (4)$$

which evaluates to 0.9387 meV for InAs using the band parameters of Table I.^{11,21}

The exact eigenstates of H_s can be used to solve the smaller contribution H_d in Eq. (1) by second-order perturbation theory. The $1s$ ground-state exciton perturbation to the effective Rydberg of Eq. (4) is given by

$$\Delta E_d(1s) = -\frac{4}{5} \left[8 \left(\frac{\mu_0}{\mu_1} \right)^2 + \left(\frac{\mu_0}{\mu_2} \right)^2 \right] \left(\sum_{n=3}^{\infty} \frac{|I_n|^2}{1-1/n^2} + \int_0^{\infty} \frac{|I_k|^2}{1+k^2} dk + \sum_{n=3}^{\infty} \frac{|I_n|^2}{\Delta+1-1/n^2} + \int_0^{\infty} \frac{|I_k|^2}{\Delta+1+k^2} dk \right), \quad (5)$$

$$I_n = \int_0^{\infty} R_{n2}(r)(r+r^2)e^{-r} dr, \quad (6)$$

where R_{n2} are normalized hydrogenic radial functions, and k^2 is the energy for continuum states. μ_1 and μ_2 are masses related to the Luttinger parameters, as defined by Balderschi and Lipari.⁷ The integrals in Eq. (5) represent the summation over continuum states. The spin-split-off band energy in InAs is ~ 400 times larger than the effective Rydberg, so the last two terms in Eq. (5) which represent the contributions to the perturbation from the spin-split band are negligible.

Since InAs has a zinc-blende structure, there is in principle an additional contribution to the Hamiltonian for a diamond lattice, Eq. (1),

$$\Delta E_p(1s) = -\frac{9}{4} \left(\frac{\mu_0}{\mu_3} \right)^2, \quad (7)$$

where

$$\mu_3 = \frac{1}{2} \frac{\mu_0 e^2}{4\pi\epsilon_r\epsilon_0\hbar^2} \frac{m_0}{\sqrt{\gamma_3^2 - \gamma_2^2}}, \quad (8)$$

but, for InAs, μ_3 is extremely large and the effect of Eq. (7) ($\sim 10^{-17}$ effective Rydbergs) is quite negligible.

Using Luttinger parameters which fit very well with magnetoabsorption data for InAs,¹² we calculate the zero-field exciton binding energy from Eqs. (1), (4), and (5) to be 1.0 meV. This value is roughly half of previously published theoretical estimates^{7,22} based on early materials parameters. For example, the older exciton binding-energy value of 1.8 meV (Ref. 7) was based on a dielectric constant of 11.8, whereas our present calculation is based on the more recent value of 15.15.^{11,21} The older exciton binding-energy value has recently been used successfully to interpret magnetophotoluminescence data of an InAs epilayer,¹⁷ although, as discussed below, this analysis alone is not a particularly sensitive measure of the free-exciton binding energy.

B. Shift of magnetoexciton at high magnetic field

In the parabolic-band approximation the effective-mass Hamiltonian in spherical coordinates for an exciton in a magnetic field reads

$$\left[-\frac{\hbar^2}{2\mu} \nabla^2 - \frac{ie\hbar}{2} \left(\frac{1}{m_e} - \frac{1}{m_h} \right) B r \times \nabla + \frac{e^2}{8\mu} (B \times r)^2 - \frac{e^2}{4\pi\epsilon_0\epsilon_r r} \right] U_n(r) = E_n U_n(r), \quad (9)$$

where μ is the reduced mass of the electron and hole and the other symbols have their usual meaning. For $1s$ excitons the orbital angular momentum is zero and the second term on the left-hand side (LHS) of Eq. (9) is therefore zero. In the high-field limit, Eq. (9) corresponds to the Hamiltonian for free-carrier Landau levels where the last term on the LHS can be treated as a perturbation due to the magnetoexcitonic binding energy. This is valid as long as the cyclotron energy is much larger than the free exciton binding energy, i.e.,

$$\gamma = \frac{(4\pi\epsilon_0\epsilon_r)^2 \hbar^3 B}{\mu^2 e^3} \gg 1. \quad (10)$$

In this high-field regime, Eq. (9) becomes separable in cylindrical coordinates, with one equation representing the rapid cyclotron motion perpendicular to the magnetic field (which has eigenstates corresponding to Landau levels) and a Hamiltonian in z representing the exciton motion parallel to the field.²³ In the adiabatic method of Elliot and Loudon,²³ magnetoexciton binding-energy eigenvalues are obtained by averaging the exciton potential along z over the wave functions for the cyclotron x - y motion.^{24,25}

Later calculations by Altarelli and Lipari⁹ extended the adiabatic scheme to include the degeneracy and anisotropy of the valence band. Excellent agreement between Altarelli and Lipari's⁹ and Weiler's²⁶ theory, and experimental magnetoabsorption spectra of InSb,²⁷ was found. The high-field magnetoexciton binding energy can be described accurately by²⁶

$$E_B(n) \cong 1.6R \left[\frac{\gamma}{2n+1} \right]^{1/3}, \quad (11)$$

where n is the conduction-band Landau-level index, R is the zero-field exciton binding energy, and γ is defined by Eq. (10). Using this simple analytical expression in the case of InSb gives excellent agreement between the theoretical energy of the magnetoexciton transition [deduced by subtracting Eq. (11) from the predicted band-to-band free Landau-level transition energies] and published magneto-PL measurements.²⁸

A theoretical description of the band-to-band transitions between the free-carrier Landau levels in the absence of the excitonic interaction was derived²⁹ by modifying the Luttinger-Kohn Hamiltonian²⁰ and treating the conduction band together with the degenerate valence band, and adding the magnetic vector potential to the momentum operator to give an 8×8 effective mass matrix. The resulting envelope functions are simple harmonic. For the Faraday configuration, transition selection rules dictate that absorption transitions fall into two sets: the "a" set being spin-up valence band to spin-up conduction band states of Landau index $n+1$ or $n-1$; and the corresponding "b" set linking spin-down states, i.e.,

$$\begin{aligned} a(n)a^c(n+1), & \quad a(n)a^c(n-1), \\ b(n)b^c(n+1), & \quad b(n)b^c(n-1). \end{aligned} \quad (12)$$

The zero-field band gap can be determined by extrapolating the numerous Landau transitions to the single zero-field energy in the normal Fan diagram,¹² and this model has recently been used to successfully fit to the magneto-

absorption data for a set of MBE InAs_{1-x}Sb_x samples to extract the alloy dependence of the various band parameters.¹² For narrow-gap materials, where the exciton binding energy is small, this Pidgeon-Brown model gives a good description of the Landau-level shifts with field, particularly for the higher Landau levels where the excitonic perturbation decreases like Eq. (11). The full 8×8 matrix Hamiltonian calculations²⁹ are lengthy, but, in the limit where E_g is much greater than the cyclotron energy, the conduction-band shift can be well approximated by²⁶

$$E[a^c(n)] \cong E_g + (n + \frac{1}{2})\hbar\omega_c + \frac{1}{2}g_c\mu_B B, \quad (13)$$

$$E[b^c(n)] \cong E_g + (n + \frac{1}{2})\hbar\omega_c - \frac{1}{2}g_c\mu_B B, \quad (14)$$

where ω_c is the cyclotron energy, g_c the electron g factor, and μ_B the Bohr magneton. In the valence bands, the shifts of the spin-up and spin-down heavy-hole energies are²⁶

$$\begin{aligned} E[a(n)] \cong & \frac{-\hbar e B}{m_0} [(n + \frac{1}{2})\gamma_1 - \gamma_2 + \frac{1}{2}\kappa + (\frac{5}{8} + f)q] \\ & + [(\gamma_1 - (n + \frac{1}{2})\gamma_1 - \kappa - \frac{1}{2}(\frac{9}{2} - f)q)^2 \\ & + 3n(n+1)\gamma_3^2]^{1/2}, \end{aligned} \quad (15)$$

$$\begin{aligned} E[b(n)] \cong & \frac{-\hbar e B}{m_0} [(n + \frac{1}{2})\gamma_1 + \gamma_2 - \frac{1}{2}\kappa + (\frac{5}{8} + f)q] \\ & + [(\gamma_1 + (n + \frac{1}{2})\gamma_1 - \kappa - \frac{1}{2}(\frac{9}{2} - f)q)^2 \\ & + 3n(n+1)\gamma_3^2]^{1/2}, \end{aligned} \quad (16)$$

where the parameters, γ_1 , γ_2 , γ_3 , q (see Table I), and f are those originally defined by Luttinger and Kohn.²⁰ The magnetic shifts described by Eqs. (13), (14), (15), and (16) agree very well with the predictions of the full Pidgeon-Brown model calculations. We compare for example, the predictions for the $a^-(2)a_c(1)$ transition (the second spin-up heavy hole to second spin-up electron Landau level) which is much higher in energy than the exciton transition of this present study, and where nonparabolicity effects are expected to be more pronounced. At a field strength of 8 T for the $a(2)a_c(1)$ transition in InAs, we find only a 1.5-meV discrepancy between the full Pidgeon-Brown matrix calculation and the calculation based on the simpler expressions of Eqs. (13) and (15). We also find that Eqs. (13)–(16) give an excellent fit to published magneto-PL spectra²⁸ of InSb, where nonparabolicity effects are even greater than in InAs over the field strengths investigated in this study.

The two lowest allowed heavy hole to conduction band transitions are plotted in Fig. 2 (curves a and b). These free-carrier Landau-level transitions extrapolate to a zero-field band-gap energy determined by the addition of the 1.0-meV zero-field exciton binding energy to the experimentally measured zero-field exciton peak position of Fig. 1. Curve d in Fig. 2 is the predicted $1s$ heavy-hole exciton transition using Eq. (11), assuming no spin splitting of the electron and valence-band states: it represents the average of the Zeeman spin-split curves c and e , and lies very close to our experimentally measured exciton peak position. This is a further verification of the validity of our zero-field exciton binding

energy value, since it is this binding energy that is used to determine the zero-field band gap from the experimental absorption peak. This band-gap value is then used to calculate the Landau-level energies and hence the magnetoexciton transitions at high field through Eq. (11).

The observed broadening of the absorption peak (Fig. 1) at high magnetic field is consistent with the calculated separation of the two spin split states. The slope in the experimental points can be approximated by

$$\Delta E = \frac{\hbar e \Delta B}{2\mu^*}. \quad (17)$$

Applying this to the high-field portion of Fig. 1 yields μ^* , the exciton reduced mass as $0.025m_0$, rather less than the value of $0.031m_0$ seen in magneto-PL measurements.⁸ In the derivation of this latter value an infinite hole mass was initially assumed, but a later parabolic-band analysis³⁰ concluded that the field shifts were still much less than would be expected theoretically, i.e., that this electron mass value was anomalously high. The discrepancy was later treated by the inclusion of conduction-band nonparabolicity,³¹ although the free-floating nonparabolicity parameter resulting from the fit was roughly twice the literature values obtained from cyclotron-resonance³² measurements.

The inclusion of spin-splitting effects, however, can resolve this remaining discrepancy since, as discussed in Sec. III, PL spectra are likely to be dominated by only the lowest allowed transitions, in this case the spin-up electron to heavy-hole exciton transition of Fig. 2 (curve e). We find, for example, that differentiating Eqs. (13) and (15) and applying (17) yields an apparent reduced mass of $0.03m_0$ for this transition, in good agreement with the $0.031m_0$ observed in Ref. 8.

It should also be remembered that impurity states are likely to influence the excitonic recombination features observed in PL measurements. PL lines initially assigned as free-exciton transitions in InAs,³³ for example, have been recently reassigned as donor bound-exciton transitions.³⁴ The binding of excitons to impurities will cause an increase in the apparent reduced effective mass extracted from the PL data using Eq. (17), since impurity states have similar hydrogenic eigenstates to an exciton and hence also have lower field shifts than band-to-band transitions. This, together with the neglect of spin splitting of conduction- and valence-band states, may lead to an overestimate of the free-exciton binding energy if expression (11) is applied to experimental PL data.

The quality of InAs epilayers has now reached the stage where PL of donor and acceptor bound excitons can be observed,^{33,34} as well as impurity-shifted cyclotron-resonance lines.^{10,14} Clearer identification of these impurities would facilitate an understanding between the free- and bound-exciton binding energies in InAs, but the unknown central cell chemical shifts of these impurities have a crucial influence on the binding energy, and make such an analysis difficult at present.

V. CONCLUSIONS

A value of 1.0 meV for the exciton binding energy of InAs is reported. This value is consistent with the observed

energy shift of the exciton at high magnetic field.

From the predicted value of the zero-field exciton binding energy, the Landau transitions extrapolate to a zero-field value of 419.2 meV, in close agreement with previously reported band-gap values of 420 meV in high-purity InAs epilayers.³⁵ The carrier densities in our samples are very low, certainly below $5 \times 10^{14} \text{ cm}^{-3}$, and hence the influence of impurities in our spectra are negligible. The close fit between the experimental data and predicted free-exciton transition at high field also corroborates our value for the exciton binding energy. The clear observation of the free-exciton absorption

even at low field in spite of large defect densities, further supports the thesis that InAs is unique among III-V semiconductors in that point defects are resonant with the conduction band,¹³ and have little effect on optical transitions.

ACKNOWLEDGMENTS

We would like to thank Ian Ferguson for the growth of the sample, and Linda Hart for x-ray-diffraction measurements and for valuable discussions of the InAs crystal structure.

-
- ¹K. L. Vodopyanov, H. Graener, C. C. Phillips, and T. J. Tate, *Phys. Rev. B* **46**, 13 194 (1992).
- ²S. Kalem, J. I. Chyi, and H. Morkoç, *Appl. Phys. Lett.* **53**, 1647 (1988).
- ³P. J. P. Tang, M. J. Pullin, S. J. Chung, C. C. Phillips, R. A. Stradling, A. G. Norman, Y. B. Li, and L. Hart, *Semicond. Sci. Technol.* **10**, 1177 (1995).
- ⁴P. J. P. Tang, M. J. Pullin, S. J. Chung, C. C. Phillips, R. A. Stradling, A. G. Norman, Y. B. Li, and L. Hart, *SPIE Int. Soc. Opt. Eng.* **2397**, 389 (1995).
- ⁵W. Dobbelaere, Ph.D. thesis, Katholieke Universiteit Leuven, 1992.
- ⁶W. L. Walukiewicz, in *Chemistry and Defects in Semiconductor Heterostructures*, edited by M. Kawabe, T. D. Sands, E. R. Weber, and R. S. Williams, MRS Symposia Proceedings No. 148 (Materials Research Society, Pittsburgh, 1989), p. 137.
- ⁷A. Balderschi and N. Lipari, *Phys. Rev. B* **3**, 439 (1971).
- ⁸S. R. Kurtz, R. M. Biefeld, and L. R. Dawson, *Phys. Rev. B* **51**, 7310 (1995).
- ⁹M. Altarelli and N. O. Lipari, *Phys. Rev. B* **9**, 1733 (1974).
- ¹⁰P. D. Wang, S. N. Holmes, Tan Le, R. A. Stradling, I. T. Ferguson, and A. G. de Oliveira, *Semicond. Sci. Technol.* **7**, 767 (1992).
- ¹¹*Semiconductors, Physics of Group IV Elements and III-V Compounds*, edited by K.-H. Hellwege and O. Madelung, Landolt-Börnstein, New Series, Group III, Vol. 17, Pt. a (Springer-Verlag, Berlin, 1982).
- ¹²S. N. Smith, C. C. Phillips, R. H. Thomas, R. A. Stradling, I. T. Ferguson, A. G. Norman, B. N. Murdin, and C. R. Pidgeon, *Semicond. Sci. Technol.* **7**, 900 (1992).
- ¹³W. L. Walukiewicz, *Phys. Rev. B* **37**, 4760 (1988).
- ¹⁴S. N. Holmes, R. A. Stradling, P. D. Wang, R. Droopad, S. D. Parker, and R. L. Williams, *Semicond. Sci. Technol.* **4**, 303 (1989).
- ¹⁵P. J. P. Tang, C. C. Phillips, and R. A. Stradling, *Semicond. Sci. Technol.* **8**, 2135 (1993).
- ¹⁶K. L. Vodopyanov, H. Graener, C. C. Phillips, and T. J. Tate, *J. Appl. Phys.* **73**, 627 (1993).
- ¹⁷S. R. Kurtz and R. M. Biefeld, *Appl. Phys. Lett.* **66**, 364 (1995).
- ¹⁸M. Altarelli and N. O. Lipari, *Phys. Rev. B* **7**, 3798 (1973).
- ¹⁹S. B. Nam, D. C. Reynolds, C. W. Litton, R. J. Almassy, and T. C. Collins, *Phys. Rev. B* **13**, 761 (1976).
- ²⁰J. M. Luttinger and W. Kohn, *Phys. Rev.* **97**, 869 (1955).
- ²¹B. R. Nag, *Appl. Phys. Lett.* **65**, 1938 (1994).
- ²²A. V. Varfolomeev, R. P. Seisyan, and R. N. Yakimova, *Fiz. Tekh. Poluprovodn.* **9**, 804 (1975) [*Sov. Phys. Semicond.* **9**, 530 (1975)].
- ²³R. J. Elliot and R. Loudon, *J. Phys. Chem. Solids* **15**, 196 (1960).
- ²⁴O. Akimoto and H. Hasegawa, *J. Phys. Soc. Jpn.* **22**, 181 (1967).
- ²⁵R. J. Elliot and R. Loudon, *J. Phys. Chem. Solids* **8**, 382 (1959).
- ²⁶M. H. Weiler, in *Defects, (HgCd)Se, (HgCd)Te*, edited by R. K. Willardson and A. C. Beer, *Semiconductors and Semimetals* Vol. 16 (Academic, New York, 1981), p. 119.
- ²⁷E. J. Johnson, *Phys. Rev. Lett.* **19**, 352 (1967).
- ²⁸R. D. Grober and H. D. Drew, *Phys. Rev. B* **44**, 13 374 (1991).
- ²⁹C. R. Pidgeon and R. N. Brown, *Phys. Rev.* **146**, 575 (1966).
- ³⁰S. K. Lyo and S. R. Kurtz, *Phys. Rev. B* **52**, 14 582 (1995).
- ³¹G. M. Sundaram, R. J. Warburton, R. J. Nicholas, G. M. Summers, N. J. Manson, and P. J. Walker, *Semicond. Sci. Technol.* **7**, 985 (1992).
- ³²G. M. Sundaram, R. J. Warburton, R. J. Nicholas, G. M. Summers, N. J. Manson, and P. J. Walker, *Semicond. Sci. Technol.* **7**, 985 (1992).
- ³³Y. Lacroix, S. P. Watkins, C. A. Tran, and M. L. W. Thewalt, *Appl. Phys. Lett.* **66**, 1101 (1995).
- ³⁴S. P. Watkins, C. A. Tran, G. Soerensen, H. D. Cheung, R. A. Ares, Y. Lacroix, and M. L. W. Thewalt, *J. Electron. Mater.* **24**, 1583 (1995).
- ³⁵C. R. Pidgeon, D. L. Mitchell, and R. N. Brown, *Phys. Rev.* **154**, 737 (1967).